International Journal of Advanced Trends in Engineering and Technology (IJATET)
Impact Factor: 5.665, ISSN (Online): 2456 - 4664
(www.dvpublication.com) Volume 2, Issue 2, 2017

INVESTIGATION ON GROWTH AND CHARACTERIZATION OF TETRAKIS-THIOUREA NICKEL SULPHATE CRYSTALS

U. Rajesh Kannan*, G. Narayanasamy*, S. Subramanian & P. Selvarajan*****

* Department of Physics, Kamaraj College, Tuticorin, Tamilnadu
** Department of Physics, MDT Hindu College, Tirunelveli, Tamilnadu
*** Department of Physics, Aditanar College of Arts and Science, Tiruchendur, Tamilnadu

Cite This Article: U. Rajesh Kannan, G. Narayanasamy, S. Subramanian & P. Selvarajan, "Investigation on Growth and Characterization of Tetrakis-Thiourea Nickel Sulphate Crystals", International Journal of Advanced Trends in Engineering and Technology, Volume 2, Issue 2, Page Number 185-193, 2017.

Abstract:

Nonlinear optical (NLO) crystals are classified into organic, inorganic and semiorganic crystals and these crystals are used in the fields of optical communication, optical computing, frequency doubling, optical data processing and opto electronics. In this work a semi-organic crystal namely tetrakis-thiourea nickel sulphate (TTNS) crystal was prepared. Slow evaporation technique was adopted to grow the single crystals of tetrakis-thiourea nickel sulphate after the growth period of 25 days. Bulk crystals were harvested from the supersaturated solution at room temperature. The harvested crystals have been subjected to various characterization techniques like XRD, FTIR, FT-Raman, and TG/DTA, Microhardness test, spectral, SHG, Z-scan and dielectric studies. The obtained results are presented and discussed.

Key Words: Single Crystal, Solution Method, XRD, FTIR, SHG, TG/DTA, NLO, Dielectrics, FT-Raman, Microhardness & Z-scan

1. Introduction:

Nonlinear optical (NLO) materials are the materials in which light waves can interact with each other and they have an impact on frequency conversion, laser, telecommunication, optical computing and data storage technology. Particularly they have gained considerable attention due to their practical application in the extension of the limited and fixed frequency outputs available from lasers **[**1-3**].** Thiourea is one of the few simple organic compounds having high crystallographic symmetry. It crystallizes in the rhombic bipyramidal division of the system and behaves as a good ligand.Thiourea is an interesting inorganic matrix modifier due to its large dipole moment and its ability to form an extensive network of hydrogen bonds **[**4, 5**].** The NLO properties of metal complexes of thiourea depend upon both organic and inorganic compounds to contribute specifically to the process of second harmonic generation **[**6-10**].** Nickel sulfate is a common source of the Ni^{2+} ion for electroplating and it has excellent mechanical and thermal properties **[**11, 12]. In this work, thiourea has been combined with nickel sulfate to form tetrakis-thiourea nickel sulfate (TTNS) crystals. The single crystals of TTNS have been grown by solution method with slow evaporation technique.

2. Experimental Method:

2.1 Synthesis and Crystal Growth:

Tetrakis-thiourea nickel sulphate (TTNS) crystals have been prepared by slow evaporation technique. The TTNS salt was synthesized by dissolving nickel sulphate and thiourea in the ratio 4:1 in deionized water. The synthesized salt was purified by successive recrystallization and utilized for the growth of TTNS crystals. After recrystallization, the salt of TTNS was dissolved in water to prepare the saturated solution, stirred well for about 2 hours to obtain a homogeneous mixture and the solution was filtered using a filter paper to remove the suspended impurities. Then the solution was allowed to crystallize by slow evaporation of solvent at 30 ^{o}C for about 25 days and the single crystals of good transparency were collected. The grown crystals were harvested from the aqueous growth medium after attaining a reasonable size. The photograph of the harvested crystals is shown in the figure 1.

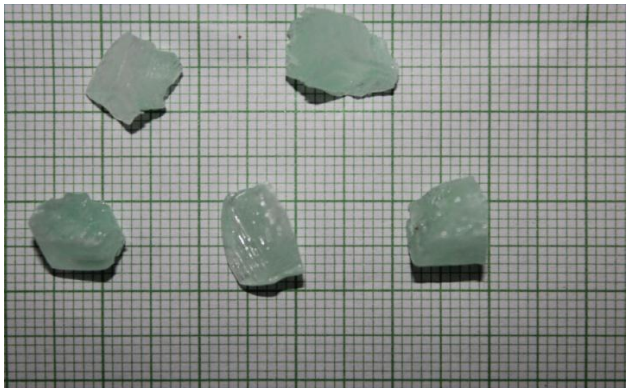

Figure 1: Photograph of the grown TTNS crystals

2.2 Characterization Methods:

Single crystal XRD data were collected using an ENRAF NONIUS CAD-4 single crystal diffractometer with MoK_α (λ = 0.71073 Å) radiation.. Powder XRD analysis was also carried out using a Rich Seifert diffractometer with Cu K_α (λ=1.54059 Å) radiation**.** A Fourier transform infrared (FT-IR) spectrometer was used to record the infrared spectrum in the wave number range 400-4000 cm^{-1} and the model of the instrument used is Perkin Elemer RXI spectrometer. The FT-Raman spectrometer was used to record the FT-Raman spectrum of the sample. The absorbance spectrum was recorded using a Perkin Elemer lambda 35 UV-vis spectrophotometer in the wavelength range of 190-1100 nm. Second harmonic generation efficiency was measured using Kurtz and Perry powder technique using Nd: YAG laser [13]. Thermal analysis was carried out using SDT Q 600V 8.3 built 101 simultaneous TG/DTA analyzer in the nitrogen atmosphere. Microhardness tester was used to measure the microhardness of the sample at different applied loads. The average of diagonal length of indentation for various applied loads with constant indentation period of 10 s was investigated. The third order NLO property of TTNS crystal was investigated using Z-scan technique and in this measurement, a He-Ne laser (λ = 632.8 nm) was used as the light source and fouced by a lens of 22.5 cm focal length. TTNS crystal of thickness 1mm was translated across the focal region along the axial direction, which was the direction of the propagation of the laser beam. The light intensities, transmitted across the sample, were measured as function of sample position in the Z-direction with respect to the focal plane either through a closed aperture (CA) or open aperture (OA) in order to resolve the nonlinear refraction and absorption coefficients[14,15].

3. Results and Discussion:

3.1 X-Ray Diffraction (XRD) Analysis:

To find the crystal structure and the lattice parameters, single crystal X-ray diffraction studies were carried out and data collected. The lattice parameters obtained are a = 19.118 (6) Å, b = 10.419 (3) Å, c =8.978 (8) Å, $\alpha = \beta = \gamma = 90^o$ and V = 1788. 33 $Å^3$.From the results, it is observed that the grown crystal crystallizes in orthorhombic crystal system with space group of $P2_12_12_1$. The powder X-ray diffraction pattern of the grown TTNS crystal was recorded by using the powder X-ray diffractometer employing CuK_α radiation and is presented in the figure 2. Appearance of sharp and strong peaks confirms the good crystallinity of the grown sample. Using INDEXING software package, the obtained XRD pattern was indexed and powder XRD data are given in the table 1.

Peak No	2θ (degrees)	Relative Intensity (%)	hkl	d (Å)
1	19.2357	5.97	220	4.574
2	20.6754	100	410	4.344
3	23.1748	22.60	212	3.786
4	25.3343	5.41	510	3.518
5	29.0935	10.70	231	3.068
6	30.3532	4.54	521	2.915
7	33.0526	4.19	303	2.709
8	36.2719	10.02	531	2.471
9	38.7913	3.22	622	2.325
10	42.5505	2.97	342	2.124
11	47.5604	3.95	450	1.910
12	54.567	2.8	932	1.680

Table 1: Powder XRD data for TTNS crystal

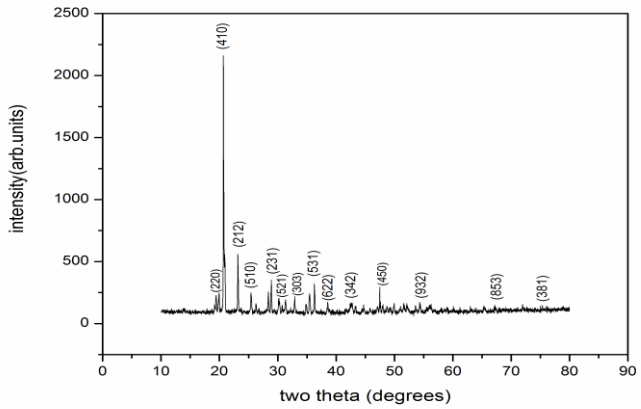

Figure 2: XRD spectrum of TTNS crystal

3.2 FTIR and FT-Raman Spectral Studies:

Spectroscopic methods such as FTIR method and FT-Raman method are used to find the molecular groups of the sample. The molecular formula of the sample can be obtained after finding the functional groups of the molecules of the sample. The presents of water of crystallization in the grown crystal can be checked by these spectroscopic methods. The FTIR spectrum was recorded using an FTIR spectrometer and FT-Raman spectrum was recorded using an FT-Raman spectrometer. The recorded FTIR spectrum and FT-Raman spectrum of TTNS crystals are shown in the figures 3 and 4. The band at 3746 cm^{-1} is corresponding to stretching vibration of OH group and the band at 3180 cm^{-1} is due to NH_2 group. The C=S stretching vibration of TTNS occurs at 1394 cm^{-1}. The vibration peak at 468 cm^{-1} confirms the presence of N-C-N deformation in the grown crystals. The peaks at 3189 cm^{-1} and 984 cm^{-1} in the FT-Raman spectrum are corresponding to NH_2 stretching and bending vibrations respectively. Using the data in the literature [16, 17], the various peaks /bands of FTIR and FT-Raman spectra have been given the frequency assignments and the complete assignments are given in the table 2.

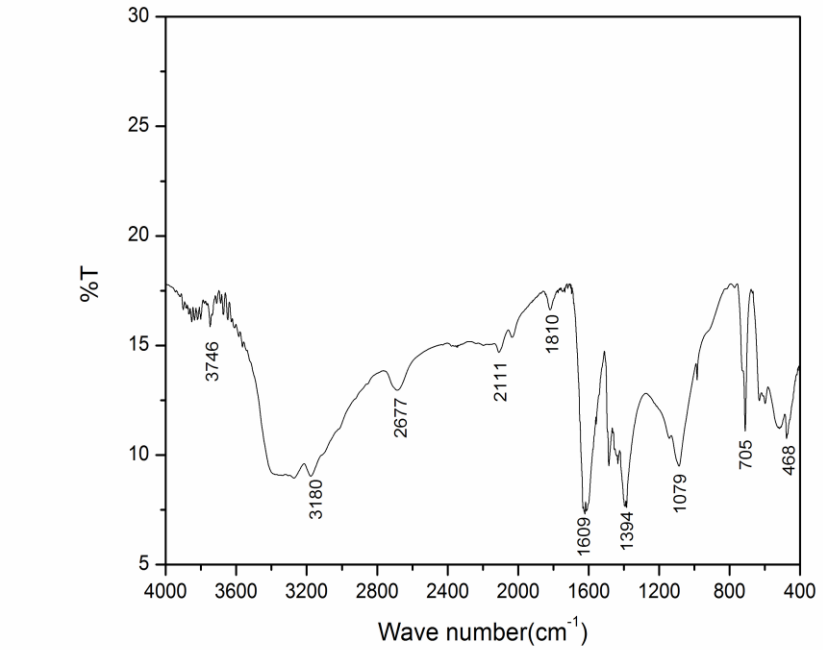

Figure 3: FTIR spectrum of TTNS crystal

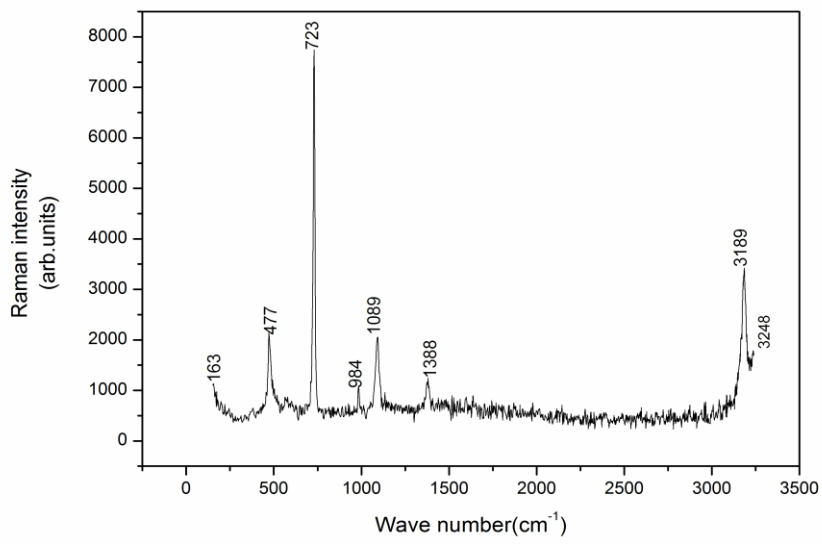

Figure 4: FT-Raman spectrum of TTNS crystal

Table 2: FTIR and FT-Raman assignments for TTNS crystal

S.No	FTIR(cm^{-1})	FT-Raman (cm^{-1})	Band Assignments
1	3746	3248	OH stretching
2	3180	3189	NH_2 Stretching
3	2677	-	O-H bending
4	2111	-	Sum tones
5	1810	-	Combinations
6	1609	-	NH_2 stretching
7	1394	1388	C= S stretching
8	1079	1089	C-N vibration
9	-	984	NH_2 deformation
10	705	723	C= S bending
11	468	477	N-C-N deformation
12	-	163	Lattice vibration modes

3.3 UV-Visible Spectral Analysis:

UV-Visible spectroscopy is an important tool to find the linear optical constants and optical band gap of the sample. The optical transmission/absorbance spectrum of the sample can be recorded using a UV-Visible Spectrophotometer in the wavelength range 200-800 nm. The recorded UV-visible-NIR absorbance spectrum of TTNS sample in this shown in the figure 5. The result shows that TTNS crystal has good transmission in the visible-NIR regions and has high absorbance at 295 nm which indicates the lower cut-off wavelength of the material. The optical band gap for the grown TTNS crystal was determined using the relation $E_g = 1242 / \lambda$. Here λ is the cut-off wavelength in nm. The calculated value of optical band gap is 4.21 eV. In the visible region of the spectrum, the sample has low absorption and it can be used for harmonic frequencies and used for NLO applications. [18, 19].

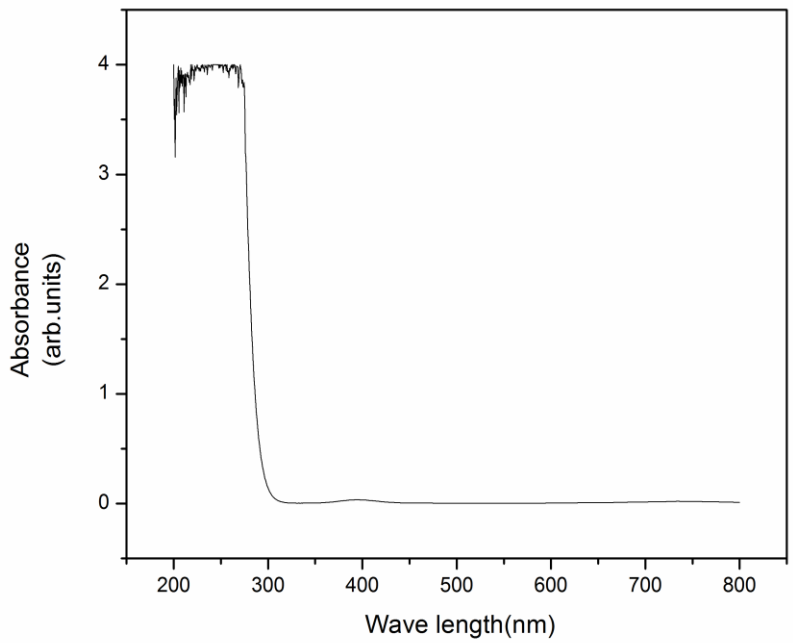

Figure 5: UV-visible-NIR spectrum of TTNS crystal

3.4 Thermal Analysis:

Thermogravimetric and Differential Thermal analyses (TG/DTA) give information regarding as the phase transition temperature, melting point and the weight loss of the grown crystal, water of crystallization and different stages of decomposition of the sample. The recorded TG'DTA thermal curves for TTNS crystal are presented in the figure 6. TG curve shows that the sample undergoes a complete decomposition between 100 ^oC to 400 ^oC. The endothermic peaks of DTA curve below 200 ^oC indicate the loss water of crystallization in the sample. The endothermic peak at 275 ^oC represents the decomposition point of the sample. The weight loss in the range 500 – 700 ^oC indicates the liberation of volatile substance and sulphur oxide. The sharpness of the endothermic peaks shows good degree of crystallinity of the sample.

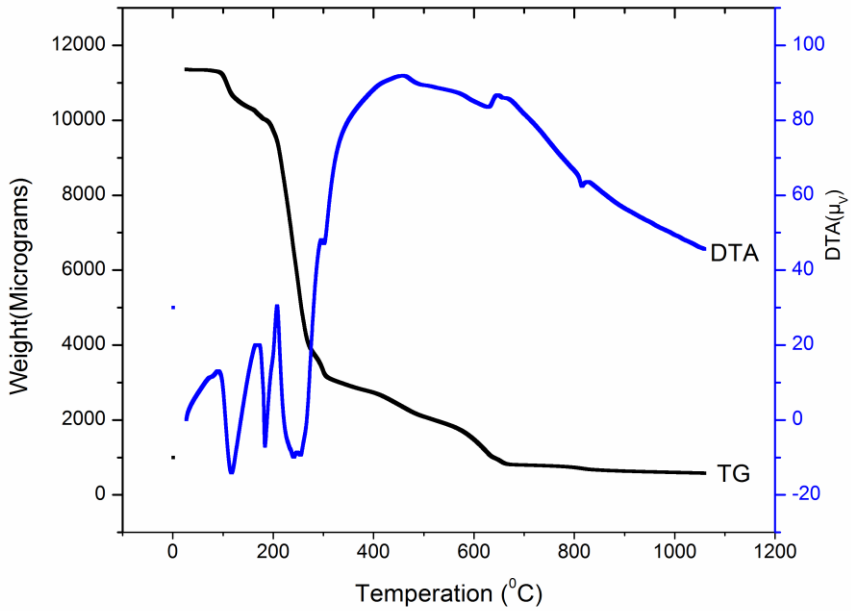

Figure 6: TG/DTA thermal curves of TTNS crystal

3.5 Second Harmonic Generation (SHG):

The Kurtz and Perry powder SHG method is used to measure the SHG efficiency of the grown crystal. In this method, powdered sample is densely packed in a capillary tube and irradiated with high intense infrared beam produced by a Q-switched Nd-YAG laser of wavelength 1064 nm with a pulse width of 8 ns and a repetition rate of 10 Hz. Potassium dihydrogen orthophosphate (KDP) crushed into sample of identical size is used as reference material. The output of laser beam having the bright green emission of wavelength 532 nm confirms the second harmonic generation output. The obtained relative SHG efficiency of TTNS crystal is 1.15. The output from SHG test confirms the nonlinear nature of the crystal.

3.6 Density of Crystal:

Floatation method was used to find the density of crystals. Liquids like xylene and bromoform are used in this experiment. After mixing the liquids xylene and bromoform in a suitable proportion in a specific gravity bottle, a small piece of the grown crystal was immersed in the liquid mixture. When the sample had attained a state of mechanical equilibrium, the density of the crystal was equal to the density of liquid mixture. The density was calculated using the relation $(w_3 - w_1) / (w_2 - w_1)$ where w_1 is the weight of the empty specific gravity bottle, w_2 is the weight of the specific gravity bottle with full of water and w_3 is the weight of specific gravity bottle full of the mixture of xylene and bromoform[20]. The determined value of the density of the grown crystal is 1.840 g/cc.

3.7 Microhardness Measurement:

Microhardness of crystal is of its capacity to resist indentation. That is hardness of a material is a measure of its resistance to local deformation. It is correlated with other mechanical properties like elastic constants and yield stress of materials. In the present study, hardness was measured using (Leitz-Wetzler) hardness tester, indentations were made on a TTNS crystal for different loads and indentation time given was 10 s. The maximum indenter load applied was 100 g .For each load, several indentations were made and the average diagonal length is used to calculate the microhardness number. The Vickers hardness for each load was determined from the formula $H_v = 1.8544\ P/d^2$, where P is the applied load in g and d is the average diagonal length in micrometer [21, 22]. Vickers hardness number is calculated and a graph has been plotted between the hardness value and the corresponding loads for TTNS crystal and it is shown in figure 7. From the results, it is observed that hardness number increases as the load is increased. Since the hardness values are more for TTNS crystal, this can be used for NLO device fabrication. Plot of log P versus log d for the sample was drawn and it is presented in the figure 8 and its slope is 5.0463 and this is equal to work hardening coefficient. Since this value is more than 1.6, this grown crystal is a soft material [23].

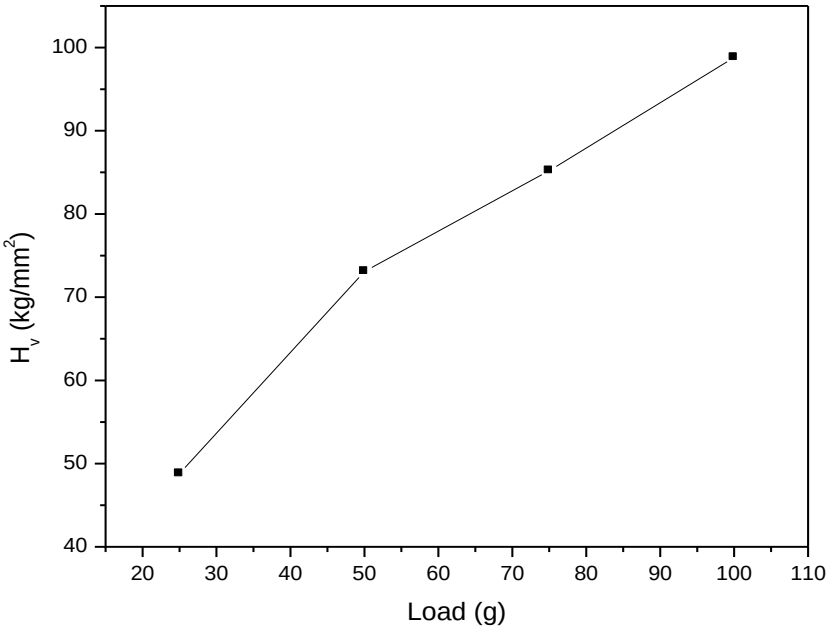

Figure 7: Plot of Vickers hardness versus applied load for TTNS crystal

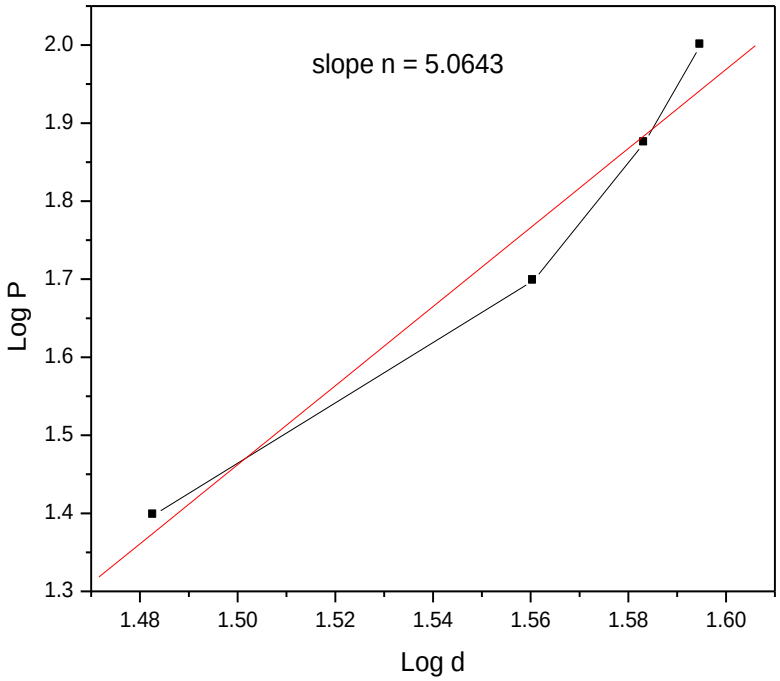

Figure 8: Plot of log P versus log d for TTNS crystal

3.8 Z- Scan Measurement:

The Z-scan is a simple and popular experimental technique to measure the intensity dependent third order nonlinear susceptibility of the materials. It allows the simultaneous measurement of both the nonlinear refractive index and the nonlinear absorption coefficient. In this method the sample is translated in the Z-direction along the axis of a focused Gaussian beam from the He-Ne laser at 632.8nm and the far field intensity is measured as a function of the sample position[**24**]. When both open aperture and closed aperture methods are used for the measurements, the ratio of the signals determines the nonlinear refraction of the sample. The Z-scan curves for the sample are shown in the figures 9. In the closed Z-scan curve, there is valley followed by a peak and it corresponds to the signature of positive nonlinearity. The calculated value of the nonlinear refractive

index (n_2) is + 6.463 x 10^{-11} m^2/W. As sample has positive refractive index, it results in focusing nature of the material. From open aperture Z-scan curve, it can be concluded that as the minimum lies beyond the focus and the nonlinear absorption is coefficient is found to be 3.658 x 10^{-4} m/W. Third order susceptibility of TTNS crystal is 5.428 x 10^{-7} esu. The value of ($\chi^{(3)}$) is found to be larger and it is due to the π electron cloud movement from the donor to acceptor which makes the molecule highly polarized. The obtained Z-scan data for TTNS crystal are given in the table 3. [25, 26]

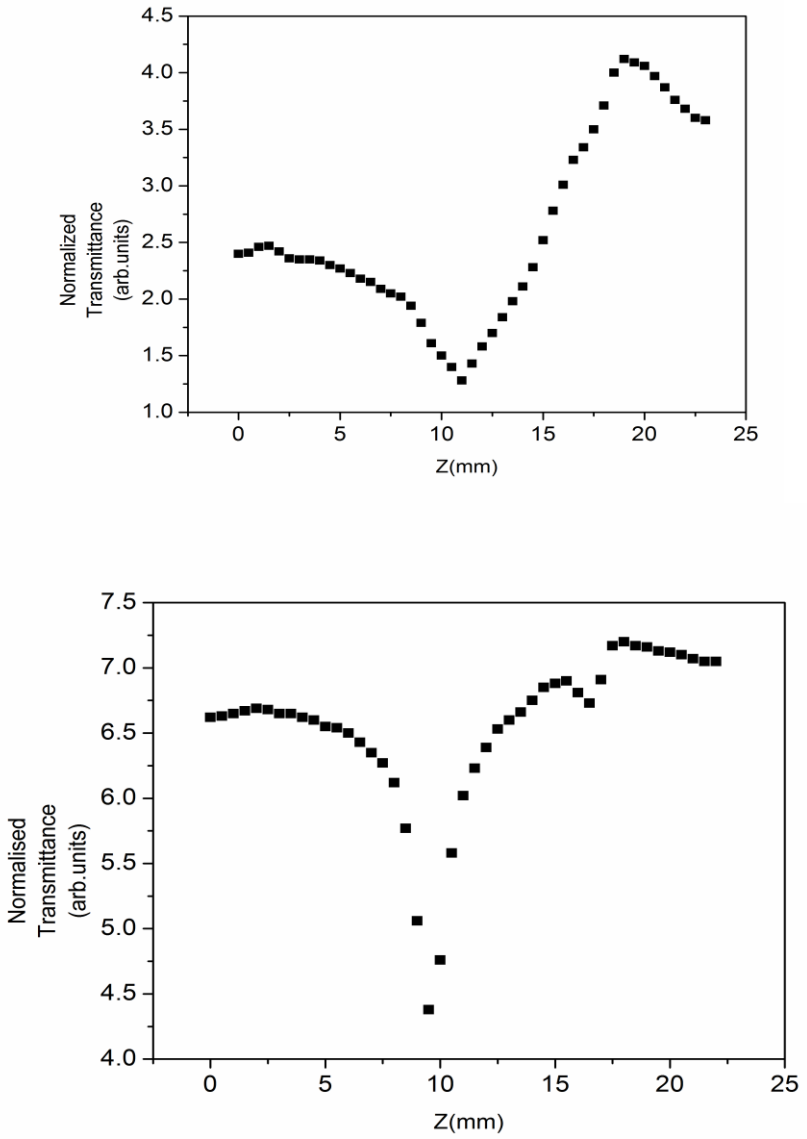

Figure 9: (a) Z-scan pattern in closed aperture. (b) Z-scan pattern in Open aperture

Table 3: Obtained data from Z-scan measurements for TTNS Crystal

Laser beam wave length (λ)	632.8 nm
Lens focal length	22.5 cm
Spot size diameter in front of the aperture (ω_a)	1 cm
Aperture radius(r_a)	4 mm
Incident intensity at the focus(z=o)	2 MW/cm^2
Effective thickness(L_{eff})	1.101 mm
Nonlinear refractive index(n_2)	+ 6.463 x 10^{-11} m^2/W.
Nonlinear absorption coefficient(β)	3.658 x 10^{-4} m/W
The third order nonlinear susceptibility ($\chi^{(3)}$)	5.428 x 10^{-7} esu

3.9 Dielectric Parameters and AC Conductivity:

The dielectric parameters like dielectric constant and loss were measured using an LCR meter at frequency of 1000 Hz at different temperatures. The variations of dielectric constant and dielectric loss with temperatures are presented in the figure 10 and it is observed that these parameters are increasing with increase

of temperature. The enhancement of capacitance provides the basic experimental method for the measurement of dielectric constant. When an electric field acts on any matter the latter dissipates a certain quantity of electrical energy that transforms into heat energy. The amount of power losses in a dielectric under the action of the voltage applied to it is commonly known as dielectric loss. [27] The lower the dielectric loss the more effective is a dielectric material. The space charge polarization depends on the purity and perfection of the material and its influence is noticeable in the low frequency region. The low value of dielectric loss at high frequency reveals the high optical quality of the crystal with lesser defects, which is the desirable property for NLO applications [28, 29] .The AC conductivity was calculated at different frequencies using the formula $\sigma_{ac} = \omega \epsilon_o \epsilon_r \tan \delta$, where ω is the angular frequency, ϵ_o is the permittivity of free space, ϵ_r is the dielectric constant and $\tan \delta$ is the dielectric loss. Figure 11 shows the plot of AC conductivity versus temperature and it is evident from the graph that the conductivity increases with temperature.

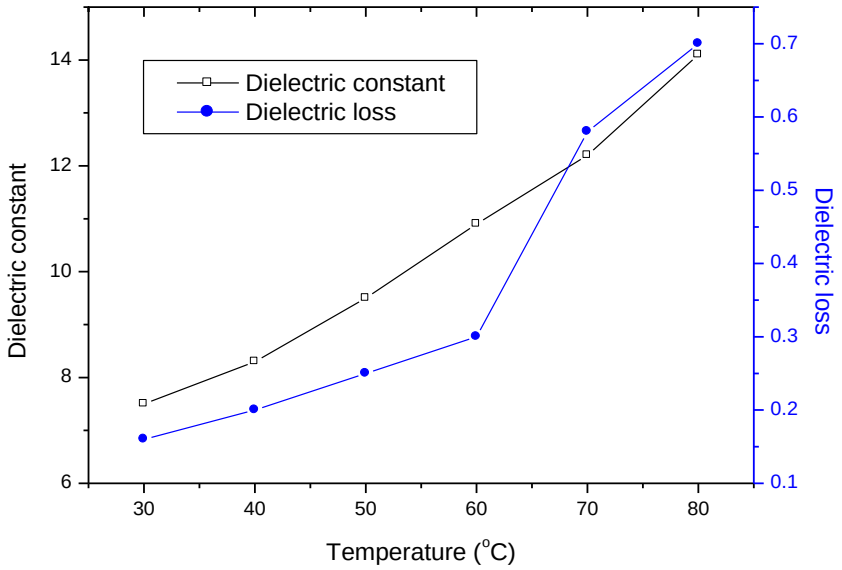

Figure 10: Variation of dielectric constant and dielectric loss with temperature for TTNS crystal

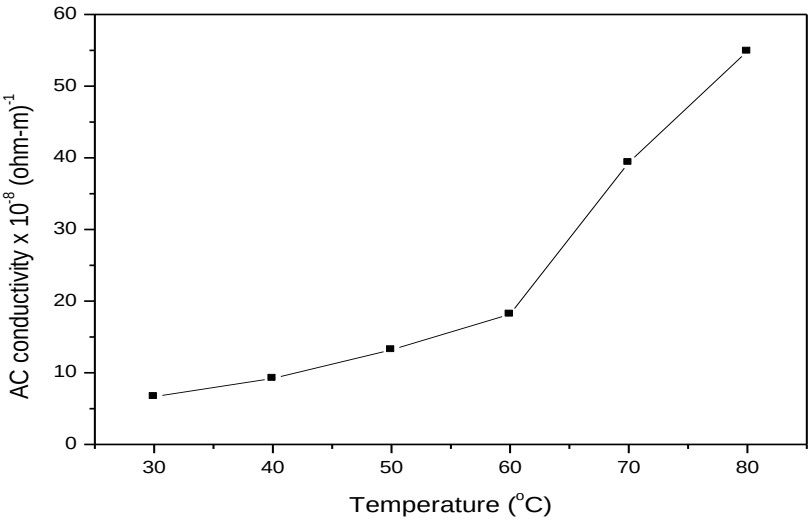

Figure 11: Variation of AC conductivity with temperature for TTNS crystal

4. Conclusions:

. Single crystals of TTNS, a new semi-organic NLO material, have been grown from aqueous solution by slow evaporation technique and the reactants used were thiourea and nickel sulfate. The X-ray diffraction studies confirm the orthorhombic structure of the grown crystal. The FTIR and FT-Raman analyses confirm the presence of various functional groups. UV-Vis NIR spectrum confirms its suitability for SHG application. TG/DTA reveals that this compound is thermally stable. SHG studies reveal that TTNS crystal is the promising

material for NLO applications. Dielectric constant and dielectric loss were measured for the sample and AC conductivity is determined at various temperatures. Third order NLO parameters for the sample were determined by Z-scan method. The mechanical strength of the sample was analysed by microhardness measurement.

5. Acknowledgements:

The research supports rendered by various research institutions such as NIT, Trichy, IIT, Madras, Annamalai University, Chidambaram, Manonmaniam Sundaranar University, Tirunelveli, St.Joseph's College, Trichy, Karunya University, Coimbatore, Crescent Engineering College, Chennai are gratefully acknowledged. The authors are thankful to the management of Aditanar College of Arts and Science, Tiruchendur and M.D.T. Hindu College, Tirunelveli and also authors thankful to the management of Kamaraj College, Tuticorin, India.

6. References:

1. Felicita Vimala. J. J. Thomas Joseph Prakash, J. Felicita Vimala et.al/Elixir Crystal growth, Volume 56 2013, 13355-13358.
2. P. Selvarajan, J. Glorium Arul raj, S. Perumal, J. Crystal Growth 311 (2009) 3835–3840
3. Revathi. V and V. Rajendran, Recent Research in science and Technology, Volume 4 (Issue 2) 2015 38-41.
4. R. Geetha kumari V. Ramakrishnan, M. Lydia Carolin, J. Kumar, Andrei Sarua, Martin Kuball, Spectrochimica Act part 73 (2009) 263-267
5. G. Senthil Murugan, P. Ramasamy, Journal of Crystal Growth 311(2009)585-588
6. Muthu. S. P. Meenakashisundaram, Journal of Crystal 352(2012)158-162
7. M. Lydia Caroline, S. Vasudevan, Materials Chemistry and Physics 113 (2009)670-674
8. R. Agilandeshwari, K. Muthu, V. Meenatchi, K. Meena, M.R ajasekar, A. Aditya Prasad, Spectrochimica Acta Part A: Molecular and Biomolecular Spectroscopy 137(2015) 383-388
9. Dhanuskodi, T. C. Sabari Girisun, Journal of Crystal Growth 330 (2011) 43-48
10. G. Bhagavannarayana. S. K. Kushwaha, S. Parthiban, G. Ajitha Subbiah, Meenakshisundaram, Journal of Crystal Growth 310 (2008) 2575- 2583
11. R. S. Sundararajan, M. Senthilkumar, C. Ramachandraja, Journal of Crysallization Process and Technology, 2013, 3,56-59
12. G. Bhagavannarayana. S. Parthiban. S. P. Meenakshisundram, J.Appl.Crystalloger,39 (2006) 784
13. S. K. Kurtz, T. T. Perry, J. Appl. Phys.39 (1968) 3798-3813.
14. Neelam Singh, B.K. Singh, Nidhi Sinha, Binary Kumar, Journal of Grystal Growth 310 (2008) 4487-4492.
15. C. Krishnan a, P. Selvarajan b, T.H. Freedac, C. K. Mahadevan Physica B 404 (2009) 289–294
16. Krishnakumar, V., Sivakumar, S. Nagalakshmi, R.," Investigation on the Physiochemical properties of the nonlinear optical crystal for blue green laser generation" Spectrochim. Acta, 2008, pp 119-124.
17. Charles J. Product, The Aldrich library of Infrared Spectra, Third Edn., Aldrich Chemical Company, INC, Milwaukee, Wisconsin
18. Rao,C.N.R., Ultraviolet and visible Spectroscopy, Chemical applications, 1975, Plenum Press.
19. Charles Kittle, Introduction to solid state physics, seventh ed., Wiley India Edition, New Delhi, 2017
20. V.V enkatramanan, Ph.D. Thesis, Indian Institute of science, Bangalore, India, 1994
21. Mott, B.WS. Micro indentation Hardness Testing (Butter worths, Scientific Publication, London), 1956
22. Sangwal, K "On the reverse indentation size effect and michrohardness measurement of solids" Mat. Chem and Phys, 63, 2000, pp 145-152.
23. Tabor, D. The Hardness of Materials,(Oxford University Press, Oxford), 1951
24. S. Shettigar, G. Umesh, K, Chandrasekaran and B. Kalluraya, Syntheitc Matals 157,142 (2007)
25. Yun Shan Zhou, En Bo Wang,and Jung Peng, Polyhedron 18,1419(1999)
26. R. A. Ganeev, I. A. Kulagin, and A.I.Ryasnyansky.Opt.Commun.229,403(2004)
27. S. Boomadevi, R. Dhanasekaran, J. Cryst. Growth 261 (2004) 70.
28. K. V. Rao and J. Smakula," Dielectric properties of cobalt oxide, nickle oxide and their mixed crystals" Journal of applied Physics, vol, 36, no.6,pp.2031-2038,1965
29. C. P. Smyth, Dielectric Behavior and Structure, McGraw-Hill, New York, 1965, pp.132